PYROMETALLURGICAL PROCESSING TECHNOLOGY DEVELOPMENT

Tadafumi KOYAMA, Masatoshi IIZUKA and Hiroshi TANAKA

Physical Chemistry Department
Central Research Institute of Electric Power Industry (CRIEPI)

1-11-1, Iwado-Kita, Komae-shi, Tokyo, 201 Japan
Tel +81.3.3480.2111 / Fax +81.3.3480.7956

ABSTRACT

Current status of development of pyrometallurgical reprocessing technology by CRIEPI was summarized. As for the electrorefining process, three different electrodes were developed for getting higher process efficiency. The prismatic anode basket which rotates during electrorefining was found to accelerate the fuel dissolution. Collection efficiency and morphology of electrodeposited uranium on steel mandrel cathode was found to vary with anode/cathode area ratio. Paddle-shaped stirrer was developed for liquid cadmium cathode which collects TRUs and uranium simultaneously. Optimal operational conditions such as cathode current density and Reynolds number of stirring were determined for collecting uranium without forming dendrite. As one of the promising way to immobilize the water-soluble salt waste, to synthesize natural occurring mineral which contain halide salt in three dimensional cage structure was proposed. Measured leachability from synthesized mineral which contained FP simulating elements was as low as those from vitrified waste form.

I. INTRODUCTION

As the most promising way to reconcile safety and economy, Central Research Institute of Electric Power Industry (CRIEPI) have been focusing on the metal fuel cycle (MFC) that originally developed by Argonne National Laboratory.[1] Pyrometallurgical reprocessing combined with injection fuel casting gives the key features such as compactness, economy and diversion resistance to the MFC[2][3]. CRIEPI has been studying MFC technology since 1986 in order to establish the technical basis of MFC[4][5][6]. Presently, applicability of pyrometallurgical technology is extended around the fuel cycle, as shown in Fig. 1. In this presentation, current status of technological development of the pyrometallurgical processing shown in Fig. 2 was summarized with emphasis on the molten salt electrorefining and waste salt immobilization.

II. ELECTROREFINING PROCESS

An operational sequence of electrorefining step is schematically shown in Fig. 3[2]. The chopped spent metal fuels or reduced oxide fuels are loaded into an anode basket, and actinides are anodically dissolved. They are reduced and collected at two types of cathodes. One is a solid cathode which collects essentially pure uranium, and another is a liquid cadmium cathode where all of the actinides (uranium, plutonium, neptunium, americium and curium) are recovered. Chemically more active FPs such as cesium, barium, cerium, etc. accumulate in the electrolyte salt in the forms of their chlorides. Less active FPs such as ruthenium and

molybdenum remain in anode basket or fall into liquid cadmium layer at the bottom of the electrorefiner. Development of each electrode in the electrorefiner is described bellow.

A. Anodic Basket for Fuel Dissolution

Anode basket should offer good contact between chopped fuel pins and fresh bulk electrolyte to prevent accumulation of oxidized actinides in the electrolyte around fuels and to facilitate transport of them[7]. Hence, two types of anode baskets with different configuration of perforated stainless steel panels were tested. Fig. 4 shows the dissolution rate of uranium segments, 10 mm in diameter and 20 mm in length, charged in these baskets. The higher anode current efficiency was obtained for the prismatic baskets arranged at right angles. It was also found that the dissolution rate is increased with faster rotation of anode baskets.

B. Solid iron cathode for uranium recovery

Due to the highest redox potential among actinides and chemically active FPs[8], uranium predominantly deposits on solid (steel) cathodes. Uranium electrotransport tests were carried out with various concentration of uranium in the electrolyte salt by using the steel cathodes in three different diameters. No deposit was collected on any cathodes at lower concentration (about 0.5 wt%), while dendritic deposits were obtained for any cathodes at higher concentration (about 2.0 wt%). Fig. 5 shows the photographs and the collection efficiency of these deposits. With using the cathode of 15 mm dia. where anode to cathode area ratio was 10.8, needles of the dendritic deposit were thin, long and likely to be broken off from the cathode. That seems to be why the collection efficiency was extremely low in this case. In the case of 30 mm dia. cathode where anode to cathode area ratio was 5.4, the dendrite was much more adherent so that the collection efficiency was quite better. When cathode area was increased further to diameter of 70 mm where anode to cathode ratio was 2.3, concentration polarization was arose at the liquid cadmium anode and the transport of uranium was interrupted, although collection efficiency was fairly good.

C. Liquid cadmium cathode for TRUs recovery

When liquid cadmium cathode is used, TRUs are collected together with uranium because of their significantly reduced chemical activities in liquid cadmium[8]. One of the problems regarding to the liquid cadmium cathode is the formation of dendritic uranium[9]. When uranium deposits faster than it is taken into the bulk cadmium, uranium dendrite forms at the surface of the cathode as shown in Fig. 6. Once the dendrite grows up, current is concentrated on it and liquid cadmium cathode works as a solid cathode where only uranium continues to deposit.

In order to avoid this problem, stirring of cathode cadmium was considered to facilitate the transport of uranium in cathode cadmium from surface to the bulk. Suitable conditions for depositing uranium on stirred liquid cadmium cathode have been studied by using the puddle shaped stirrer. Fig. 7 shows the effect of stirring with different cathode current density on dendrite formation. The height of each bar indicates how much uranium can be collected without liquid cadmium cathode before dendrite begins to grow up. It shows much

more uranium can be collected without forming dendrite with more impetuous stirring[10]. In these tests, uranium was collected up to 10 wt% into the cathode with current efficiency of approximately 100 %.

D. Computer code development for design optimization

(i) simulation of electrochemical behavior

Practically, conditions for electrorefinig operation such as composition of the spent fuel and of electrolyte salt cannot be kept constant. Hence, a computational code, TRAIL, was developed for analyses and prediction of the electrotransport behavior of elements in various condition[11]. This code employs diffusion-limited electrochemical reaction model described in Fig. 8. A comparison between actual result of the electrotransport test of uranium and plutonium reported by ANL[12] and calculation is shown in Fig. 9. Good agreement between composition of the cathode products in both cases indicates that the behavior of each element in electrorefining step can be predicted by this code.

(ii) potential distribution calculation of specific electrorefiner

Decrease of the cell resistance is necessary for developing high throughput electrorefiner. Cell resistance strongly dependent on the geometrical configuration of the electrodes in the electrorefiner. Hence, a computational code, CAMBRIA, was developed for analyses of the cell resistance of the electrorefiner with various electrode configuration.[13] This code enables to calculate the 2-dimensional potential distribution and current distribution in the electrolyte by solving the Laplace equation with using Finite Element Method. It should be noted that this code calculates the configuration resistance without polarization. As shown in Fig. 10, however, it works well for rough prediction of the cell resistance.

III. IMMOBILIZATION of SALT WASTE

Salt waste generated at electrorefining step contains much amount of chemically active FPs such as alkali, alkaline earths, and iodine in the form of halides. Because these halides are highly soluble into water, this salt has to be converted into a stable chemical form for disposal. Alkali halides and alkaline halides are, however, hard to be converted directly into oxides, and to be dissolved into bolosilicate glass in high concentration. Hence, method to immobilize waste salt has to be developed. At present, two different immobilization methods are under study in CRIEPI. One is an electrolysis of waste salt into metal and chlorine gas followed by vitrification. It is found that the use of different cathode materials made it possible to separate the radioactive elements from nonradioactive base salt. The detail of the experimental results of this method will be reported in this conference[14]. Another method is to synthesize natural occurring mineral that contains halide salt stably in it's structure from the waste salt[15]. The three dimensional sodalite structure (Fig. 11) was found to be synthesized according to the following dry reaction,

$$6NaAlO_2 + 2NaCl + 6SiO_2 \Rightarrow Na_8[(AlO_2)_6(SiO_2)_6]Cl_2, \qquad (1)$$

where a mixture of $NaAlO_2$, SiO_2 and simulated waste salt were pressed at 200 MPa and heated at a temperature of 973 - 1173 K for 50 - 100h. Products were identified as of sodalite structure by X-ray diffraction. Leachability was measured for the synthesized sodalite specimen before or after irradiation by γ-ray. As shown in Table 1, measured leachability of the relevant elements are as low as the values reported for vitrified waste form or zeolite form[16].

V. SUMMARY

Major progress and present status were summarized on electrorefining process and waste salt immobilization process. Although it is still in an early stage of development comparing to the conventional PUREX process, any problems regarding to actual application of pyrometallurgical processing technology was not found, yet. This technology was originally developed in the United States, however, CRIEPI is now planning to continue research and development activities to establish its practicability as an advanced reprocessing technology.

ACKNOWLEDGMENT

The authors wish to acknowledge the contributions from the joint study with Toshiba Corp. for electrorefining and Hitachi Ltd. for waste salt treatment. They also acknowledge the information exchange with Argonne National Laboratory about pyroprocess technology.

REFERENCES

[1] Y. I. Chang, " The Integral Fast Reactor", *J. Nucl. Technol.*, **88**, 129(1989)..

[2] J. J. Leidler et al., *Proceedings of GLOBAL'93*, 1061(1993).

[3] J. E. Battles et al., *Proceedings of RECOD'91*, **VI**, 342(1991).

[4] M. Tokiwai et al., *Proceedings of FR91*, VII12.7-1(1991).

[5] T. Nakagawa et al., *Trans. ANS*, **60**,315(1989).

[6] K. Yokoo et al., *Proceedings of PHYSOR*, **vol. 4**, pIII-41(1990).

[7] E. C. Gay et al., *Proceedings of GLOBAL'93*, Seatle, Washington, 1331(1993).

[8] T. Koyama et al., "Pyrometallurgy Data Book", CRIEPI report, T93033,(1995).

[9] ARGONNE NATIONAL LABORATORY, "CMT Annual Technical Report 1987", ANL-88-19, 95(1988).

[10] T. Koyama et al, *Proceedings of ICCT96*, Osaka, Aug. 25-30, 279(1996).

[11] T.Kobayashi et al., *J Alloys and Compounds*, **197**, 7(1993).

[12] Z. Tomczuk, *J. Electrochem. Soc.*, **139**(12), 3524(1992).

[13] T.Kobayashi et al., *J Nucl. Sci. Technol.*, **37**(1), 68(1995).

[14] Y. Sakamura et al., *Proceedings of this conference* (1996).

[15] T. Koyama et al., *Proceedings of GLOBAL'95*, Verseille, France, V2, 1744 (1995).

[16] M. A. Lewis et al., *J. Am. Ceram. Soc.*, **76**(11), 2826(1993).

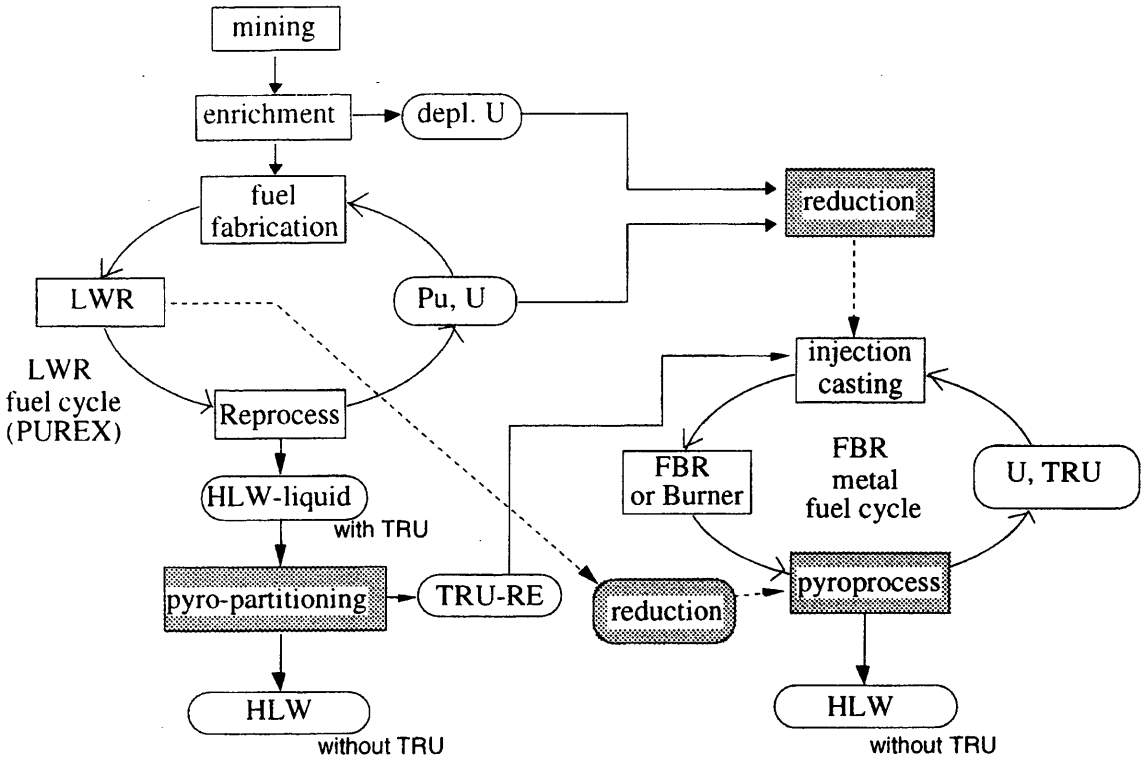

Fig. 1 CRIEPI's PYRO program in fuel cycle.

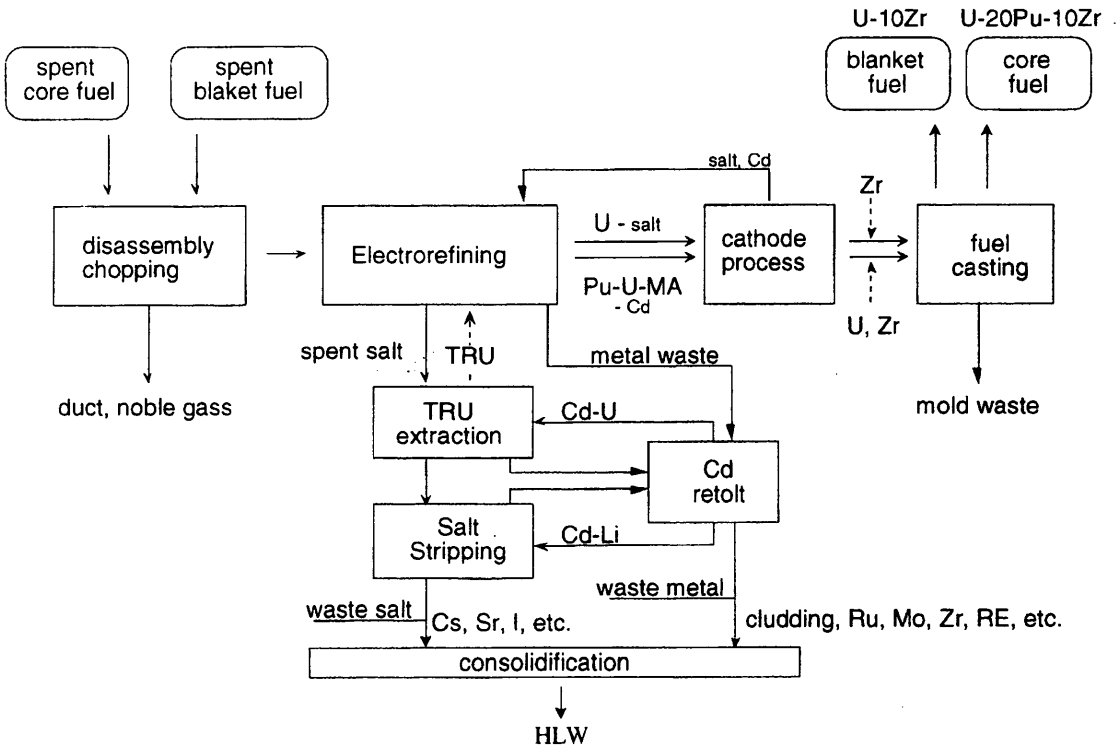

Fig. 2 Pyrometallurgical reprocessing process.

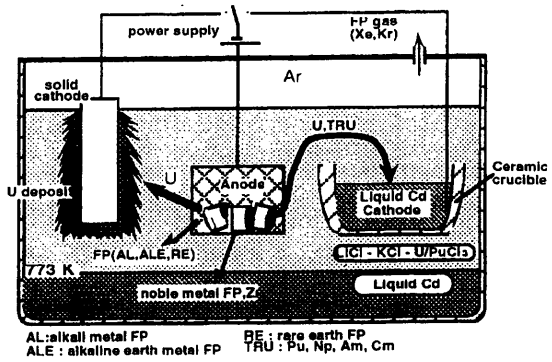

Fig. 3 Sequence of electrorefining process.

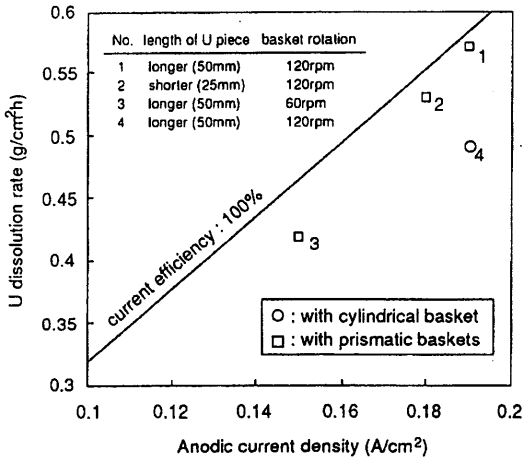

Fig. 4 U dissolution rate with different anode baskets.

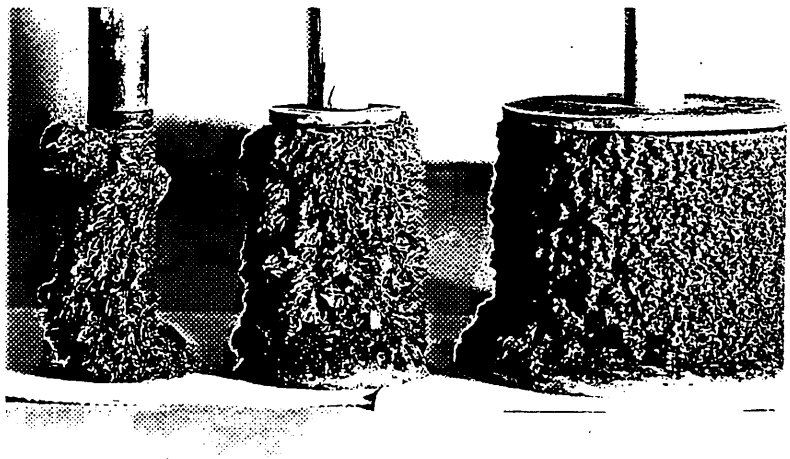

anode/cathode area ratio	10.8	5.4	2.3
collection efficiency	9.3 %	77 %	65 %

Fig. 5 Deposits on solid cathodes of different diameter.

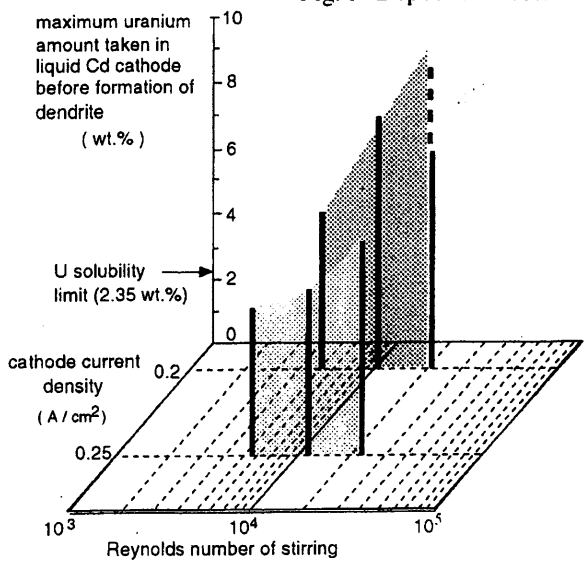

Fig. 6 Uranium dendrite on liquid cadmium cathode.

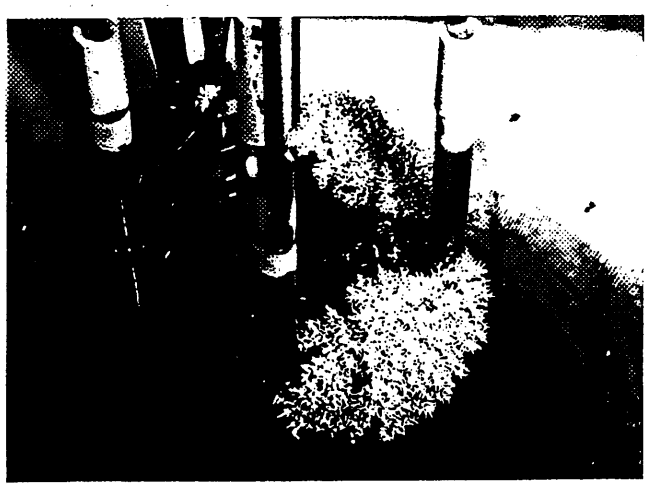

Fig. 7 Deposited U amount before dendrite iformation.

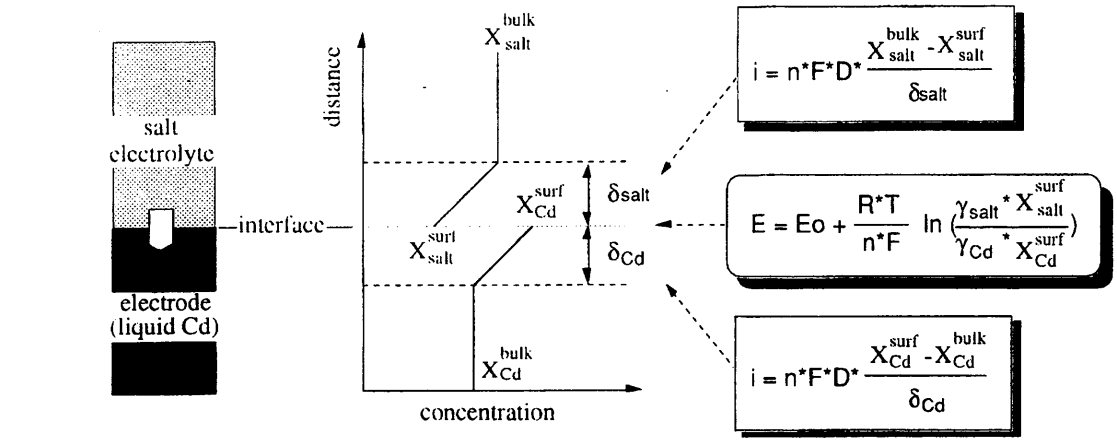

Fig. 8 Model for ectrorefining simulation code.

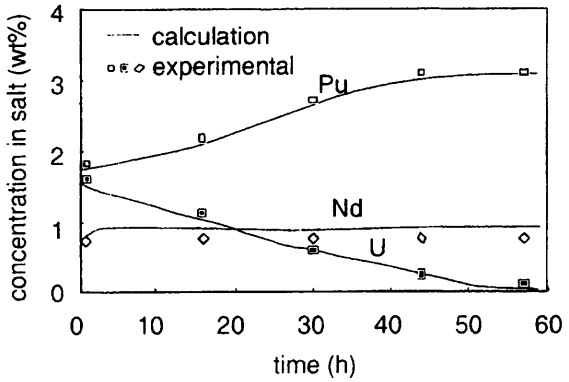

Fig. 9 Electrorefinig behavior reported by ANL.

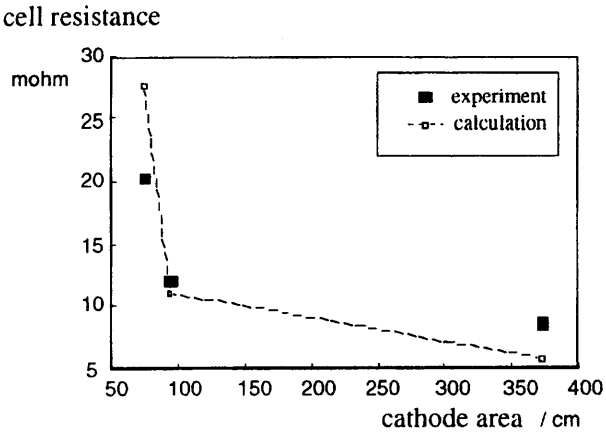

Fig. 10 Cell resistance of electrorefiner.

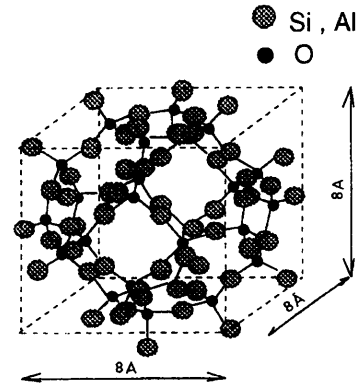

$Na_6[(AlO_2)_6(SiO_2)_6] \cdot 2NaCl$

Fig. 11 Sodalite structure with 3-D cage.

Table 1 Leachability (g/cm^2d) from sodalite, zeolite and glass.

	sodalite	zeolite *	bolo-silicate glass *
Li	0.0047	0.12	0.29
K	0.0061	0.031	0.22
Na	0.0023	0.018	0.28
Cs	0.0013	0.0066	NM
Sr	0.00035	< 1.0E-5	NM
Ba	0.000069	< 1.0E-5	NM
Al	0.0015	0.0048	0.14
Si	0.0017	0.0041	0.23
Cl	0.0022	NM	NM
I	0.0029	NM	NM

NM: not measured